ISSN No:-2456-2165 https://doi.org/10.5281/zenodo.14637043

Performance Evaluation of Underwater Wireless SAC-OCDMA System

Suman Kumar Dey[1]
Department of Electrical and Electronic Engineering
North Western University

Bithi Nahar[2]
Department of Electrical and Electronic Engineering
North Western University

Debbrota Kumar Ghuha[3]
Department of Electrical and Electronic Engineering
North Western University

Rashdul Islam[4]
Department of Electrical and Electronic Engineering
North Western University

Abstract:- This study evaluates Underwater wireless spectral amplitude-coding optical code division multiple access (SAC-OCDMA) systems bit error rate (BER) performance when employing Modified Quadratic Congruence (MQC) codes as user address sequences. Balanced detection is utilized to mitigate multi-user interference (MUI), and use constant in-phase cross-correlation values of MQC codes. BER calculations consider phase-induced intensity noise (PIIN), shot noise, and thermal noise under varying optical signal power, link distances, inclination angles, and the number of concurrent users. The performance of photodiodes and avalanche photodiodes is compared, with the latter exhibiting enhanced sensitivity and noise characteristics, facilitating the detection of weaker signals across extended distances. The system's BER is examined across various seawater forms: pure seawater, clear ocean water, and coastal ocean water. The results indicate the optimal performance of avalanche photodiodes in pure seawater.

Keywords:- *BER Performance, Spectral Amplitude Coding (SAC), Underwater Wireless OCDMA, Modified Quadratic Congruence (MQC) Codes, Multi-user Interference (MUI), Photodiode, Avalanche Photodiode*.

I. INTRODUCTION

Underwater Wireless Optical transmission (UWOC) is attracting interest due to its minimal latency, substantial bandwidth, and superior security relative to acoustic and radio frequency transmission. Acoustic waves are appropriate for long-distance communication, whereas optical and RF waves provide higher data rates over shorter distances due to attenuation. UWOC is utilized in oceanographic data acquisition, environmental surveillance, and autonomous underwater vehicles (AUVs).

Optical Code Division Multiple Access (OCDMA) improves spectral efficiency, security, and resilience by distributing data across a broader frequency spectrum through the use of coding sequences in temporal or wavelength domains. Nonetheless, OCDMA encounters obstacles such as Multi-User Interference and Phase-Induced Intensity Noise, which impair system efficacy. Spectral Amplitude Coding (SAC) OCDMA, employing Modified Quadratic Congruence (MQC) codes with balanced detection, significantly mitigates multiple access interference (MUI) and improves system stability. MQC codes, possessing excellent code weight and length characteristics, are suitable for 1D SAC-OCDMA systems. Photodiodes, particularly Avalanche Photodiodes (APDs), are essential in underwater optical wireless communication (UWOC) systems because of their ability to convert light into electrical signals with great sensitivity and rapid response. APDs function under reverse bias and utilize the photoelectric effect to attain substantial signal amplification, rendering them crucial in optical communication systems.

The exploration of underwater communication technologies uncovers a variety of challenges and innovations. A Doppler compensation system facilitates acoustic communications at a rate of 16 kbps with a signal-to-noise ratio of 11.4 dB over a distance of 200 m; however, the bandwidth is limited to 2–5 kHz for distances greater than 1 km. In underwater sensor networks, RF waves exhibit a notable increase in attenuation as temperatures rise, ranging from 145 dB at 5°C to 175 dB at 25°C. Optical communication (UWOC) utilizing LEDs has shown link distances between 10 and 30 meters, while lasers have reached 9.6 Gbps over 8 meters, though shorter ranges constrain them. A bidirectional link of 34.5 m was accomplished utilizing LED arrays; however, signal attenuation continues to pose a challenge. Recent advances encompass experiments utilizing blue lasers and turbulence analysis, emphasizing diminished signal strength under extreme conditions. Multi-input/multi-output (MIMO) systems effectively tackle turbulence-induced degradation, whereas optical code division multiple access (OCDMA) significantly improves spectral efficiency and robustness. Non-coherent SAC-OCDMA systems have attracted attention due to their cost-effectiveness, with recent investigations assessing their BER performance across different water types. This thesis investigates the effectiveness of SAC-OCDMA in underwater settings through the application of modified quadratic congruence codes (MQC), focusing on existing research gaps and assessing performance across various water types and system parameters.

ISSN No:-2456-2165 https://doi.org/10.5281/zenodo.14637043

The project focuses on creating an analytical framework to assess the bit error rate (BER) performance of an underwater wireless spectral amplitude coding optical code division multiple access (SAC-OCDMA) system that employs modified quadratic congruence (MQC) codes for user address formats. The main goals involve presenting the SAC-OCDMA system, and determining the bit error rate by taking into account phase-induced intensity noise (PIIN), shot noise, thermal noise, and the effects of optical beam absorption and scattering in seawater and atmospheric turbulence. Additionally, system performance will be analyzed across different optical power levels, link distances, inclination angles, and user counts. Furthermore, the project investigates the BER performance of photodiode and avalanche photodiode configurations in various water types (pure seawater, clear ocean water, and coastal ocean water) to determine the best parameters for improved system performance.

II. METHODOLOGY

This thesis offers an undersea wireless SAC-OCDMA structure that makes use of MQC codes for user address sequences. Additionally, the system incorporates an LED that runs at a central wavelength of 532 nm in order to limit the amount of attenuation that occurs throughout the water. To address numerous user's intervention (MUI) and reducing phase-induced depth clamor (PIIN), a balanced photo-detection technology is utilized. This technique makes use of two avalanche photodetectors (APDs) that are coupled in series. A number of parameters, including bit error rate (BER), are taken into consideration during the examination of system performance. These factors include absorption, scattering, shot noise, thermal noise, and PIIN. However, the impacts of dark current are not taken into account. under this analysis, the system is examined under a variety of seawater circumstances, including pure sea water, translucent ocean water, and seaside water. The analysis also addresses the effects of pollutants on performance. All of the research is conducted in a line-of-sight (LOS) setup, with the primary focus being on the mathematical modeling of the proposed system.

Figure 1 illustrates the conceptual layout of the expected wireless undersea SAC-OCDMA system, where Figure depicts the transmitter portion and Figure displays the receiver portion. The transmitter utilizes an LED as the optical source, functioning at a central wavelength of 532 nm and featuring a spectral bandwidth of 10 nm.

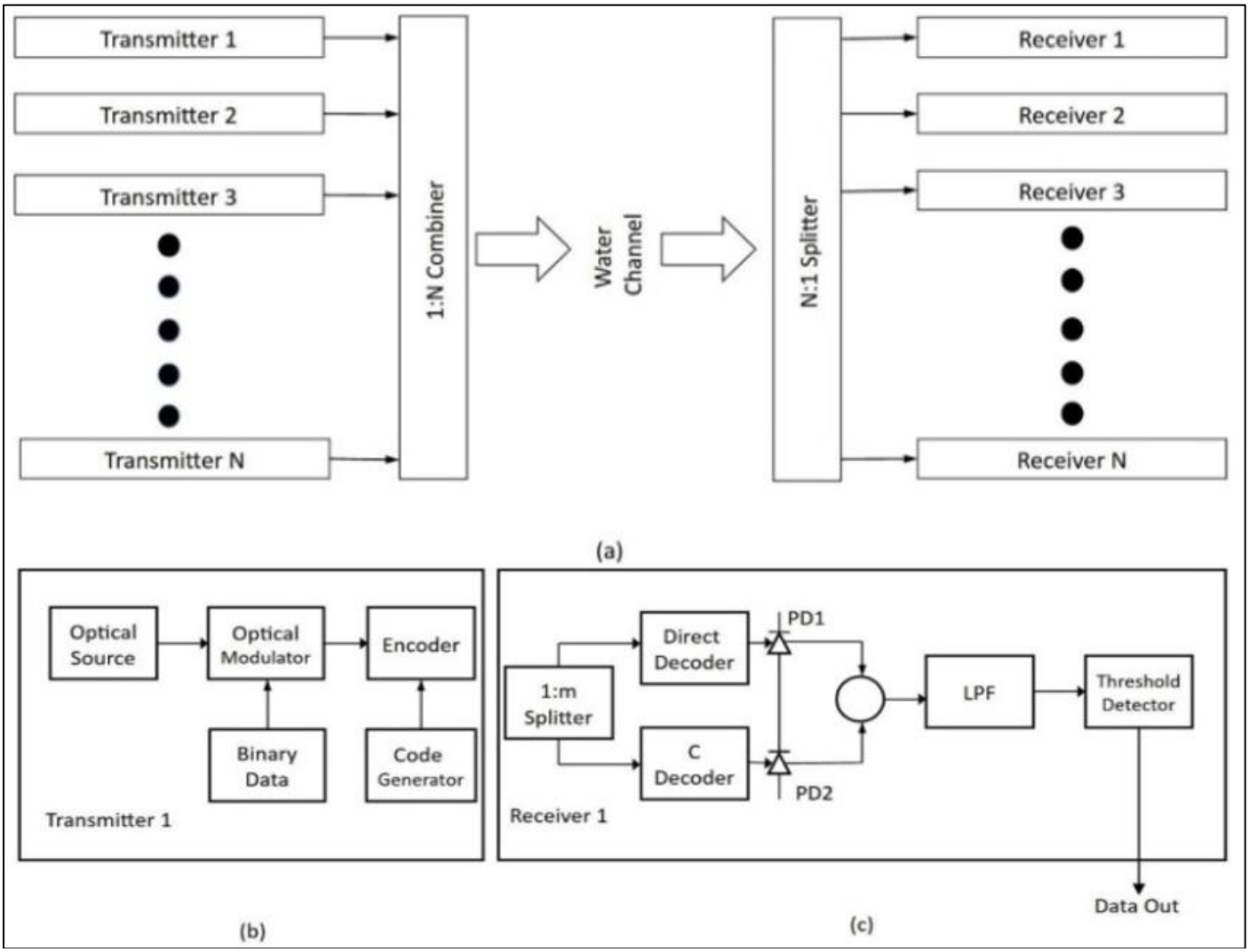

Fig 1 Abstract Diagram of Underwater Wireless SAC-OCDMA System.

ISSN No:-2456-2165 https://doi.org/10.5281/zenodo.14637043

Figure presents the abstract design of the expected underwater wireless SAC-OCDMA system, utilizing MQC codes for address sequences with \(U \) active users. The system has been streamlined to provide a detailed view of a single transmitter and receiver. At the transmitter, a broadband visual source generates vibration that are modulated with binary data, encoding a "1" with a particular spectral distribution while a "0" results in no pulse being emitted. The encoded signals are integrated and sent through a water channel. A splitter at the receiver distributes the combined signal to multiple receivers, with each signal subsequently divided into two components: one designated for decoding and the other for complementary decoding (C-decoding). The C-decoder conveys frequencies that have been dismissed by the primary decoder. The approach of balanced detection, which employs two photo detectors connected in opposition, effectively reduces multiple-user interference (MUI) by eliminating noise from unwanted users, provided that both photo detectors are subjected to the same noise levels. The resulting signal is subjected to low-pass filtering and threshold detection to retrieve the original data.

- *The subsequent subsections outline the mathematical framework of the proposed underwater SACOCDMA system. Designing underwater connections:*

To conduct an analysis of the UWOC system, it is essential to primarily consider the system's link budget equation. In a line of sight (LOS) setup, the link budget equation of a UWOC system, dependent on x, is expressed as follows [1],[2]:

$$R_{P=} T_P \eta_T \eta_R \frac{a_R \cos\theta(inc)}{2\pi L^{2[1-\cos\theta(div)]}} exp\left[-c(\lambda)\frac{L}{\cos\theta(inc)}\right]\chi \quad (1)$$

In this context, TP denotes the transmitted optical power, ηR indicates the optical efficiency of the receiver, ηT signifies the transmitter's optical efficiency, L Refers to the link distance, aR denotes the receiver's aperture area, and θdiv describes the angle of beam divergence., and θinc pertains to the inclination angle. The attenuation coefficient is denoted as c(λ):

$$c(\lambda)= \alpha(\lambda)+ \beta(\lambda) \quad (2)$$

In this equation, $\alpha(\lambda)$ denotes the coefficient of exploitation, $\beta(\lambda)$ indicates the irregular coefficient., and λ indicates the optical wavelength.

- *The Calculation of Bit Error Rate for a Photodiode:*

This system takes shot noise, thermal noise and phase-induced intensity noise into account. While the impact of the receiver's dark current has been omitted in the assessment of the BER. Assuming the noise sources are independent and follow a Gaussian distribution. The total power of the noises that affect both PDs can be represented as:

$$i_{noise}^2 = i_t^2 + i_p^2 + i_s^2 \quad (3)$$

Here, i2, i2 and i2 represent the variance of thermal noise, PIIN and shot noise respectively.

t p s

While shot noise and PIIN noise are reliant on the photo-currents of the PDs, thermal noise is not. Thermal noise can be expressed as:

$$i_t^2 = \frac{4k_c T_{no} B_w}{r_L} \quad (4)$$

Here, kc represents Boltzmann's constant, Tno denotes the absolute noise temperature of the receiver, Bw signifies the electrical bandwidth of the receiver related to noise, and rL indicates the load resistance. The discharge noise can be written as [9]

$$i_t^2 = 2_q(i_{PD1} + i_{PD1})B_w$$

$$= 2qB_w r_e R_p \left[\frac{P-1+2K}{P^2+P}\right] \quad (5)$$

In this context, $iPD1$ and $iPD2$ represent the PD1 and PD2 photocurrents, correspondingly. The prime number of MQC codes is indicated by the variable p., while q signifies the charge of an electron. Additionally, re refers to the responsively of the PDs, which can be expressed as:

$$r_e = \frac{\eta_{PD} q}{h_{v0}} \quad (6)$$

In this context, ηPD represents the quantum efficiency of the photo-detector, $v0$ denotes The core frequency of the initial broad band optical pulse, and h represents Planck's constant. The evaluation of the PIIN noise may be conducted as outlined in [9].

$$i_p^2 = (B_w i_{PD1}^2 \tau_{PD1} + B_w i_{PD2}^2 \tau_{PD1}) \quad (7)$$

In this context, $\Delta\omega$ denotes the heat source's line width. The coherence time of the optical source at PD1 is represented by $rPD1$, and the coherence time of the optical source at PD2. By substituting equations (4), (5), and (7) into equation (3), one can calculate the overall power of noise. Every user has a 50% chance of sending a "1" at any given time. Thus, the ultimate way to describe overall noise power is like this:

$$i_{noise}^2 = \frac{B_w r_e^2 R_p^{2k}}{2\Delta\omega(P+1)P^2}\left(\frac{k-1}{P} + P + k\right) + qB_w r_e R_p \left[\frac{P-1+2k}{P^2+P}\right] + \frac{4k_c T_{no} B_w}{r_L} \quad (8)$$

At the PDs' output, the regular received photocurrent can now be computed as -

$$i_{PD} = i_{PD2} - i_{PD1} = r_e \frac{R_P}{P} b \quad (9)$$

Here$b$ is a specific user's bit value that is one of two "1" or "0." The SNR of an optical system can be expressed as follows, as is well known.,

ISSN No:-2456-2165 https://doi.org/10.5281/zenodo.14637043

$$SNR = \frac{i_{PD}^2}{i_{noise}^2} \quad (10)$$

It is therefore possible to compute the system's SNR by replacing (8) and (9) in (10). Consequently, a system's BER when taking the Gaussian similarity into account can be expressed as follows:

$$BER = \frac{1}{2} erfc\left(\sqrt{\frac{SNR(\chi)}{8}}\right) \quad (11)$$

➢ *Calculation of BER (for Avalanche Photodiode):*

The BER of an optical signal, taking into account the turbulence impact, can be represented as:

$$BER_0(x) = \frac{1}{2} erfc\left(\sqrt{SNR(x)/8}\right) \quad (12)$$

The average bit error rate (BER) of an optical signal for a gamma-gamma dispersed underwater channel will be :

$$BER \int_0^{\infty} = BER_0(x)dx \quad (13)$$

The following formula serves as an illustration of the system's signal to noise ratio (SNR):

$$SNR(X) = i_{avg}^2 / i_{nois}^2 \quad (14)$$

Here, i_{nois}^2 symbolizes the overall noise power that is disrupting the system. Once more, i_{avg}, which represents the average photo-current at the output of both APDs, can be shown as [4]:

$$i_{avg} = i_{APD2} - i_{APD1} = A r_e \frac{R_P}{P} b \quad (15)$$

Here,i_{APD1} denotes the photocurrent at APD1, and i_{APD2} denotes the photocurrent at APD2. A is the APDs' gain, p is the prime number of the MQC code series, and r_e is the APDs' responsivity, while b is a bit value that can be either "1" or "0" for each user. However, [4] illustrates the overall power of noise impacting the system:

$$i_{noise}^2 = i_t^2 + i_p^2 + i_s^2 \quad (16)$$

Here, i_t^2, i_p^2 and i_s^2 *represent the variance of thermal noise, PIIN and shot noise respectively*. The thermal noise can be illustrated as [4]:

$$i_t^2 = \frac{4k_c T_{no} B_w}{r_L} \quad (17)$$

In this case, Boltzmann's constant is denoted by kc, the receiver's absolute noise temperature by T_{no}, the noise-corresponding electrical bandwidth by B_w, and the load resistance by r_L. On the other hand, shot noise variance can be represented as [4],

$$i_s^2 = 2q(i_{APD2} - i_{APD1}) B_w A^2 f_e \quad (18)$$

In this case, q stands for electron charge and A for both Si-APDs' gain. On the other hand, f_e illustrates the extra noise factor of Si-APDs in such a way that:

$$f_e = AK_e + (1 + K_e)\left(2 + \frac{1}{A}\right) \quad (19)$$

In this case, k_c is referred to as the ionization factor. The PIIN noise can now be represented as [4],

$$i_p^2 = (B_w i_{APD1}^2 \tau_{APD1} + B_w i_{APD2}^2 \tau_{APD2}) A^2$$

$$= \frac{B_w r_e^2 R_p^2 K}{2\Delta\omega(p+1)P^2}\left(\frac{K-1}{P} + P + k\right)A^2 \quad (20)$$

$\Delta\omega$ represents the thermal source line. The breadth, τ_{APD1}, indicates the optical source's coherence duration at APD1, while τ_{APD2} shows the coherence duration of the optical source at APD2. Take data bit '1', which is transmitted by every user. The possibility of each user delivering '1' is 50%. Thus, the noises resulting power can be estimated by replacing (8), (9) and (12) in (7).

$$i_{noise}^2 = \frac{B_w r_e^2 R_p^2 K}{2\Delta\omega(p+1)P^2}\left(\frac{K-1}{P} + P + k\right) + qB_w r_e R_p \left[\frac{P-1+2K}{P^2+P}\right] A^2 f_e + \frac{4k_c T_{no} B_w}{r_L} \quad (21)$$

III. RESULT AND DISCUSSION

The objective of this chapter is to elucidate the plot of the prospective system's Bit Error Rate (BER) work concerning various system parameters. In section 2.1 different water types of the system's BER performance are investigated concerning distinct system parameters. Section 2.2 discusses the impact of beam divergence angle on the system's Bit Error Rate (BER) performance. Section 2.3 addresses the calculation of the required optical power to sustain a BER of 10^-9 for individual types of water, with the selection of a BER of 10^-9 aligned with communication standards. The impact of various form of atmospheric turbulence on the BER performance is shown in section 2.4. The computation of the system's required power, considering of various levels of atmospheric turbulence, is shown in section 2.5. Section 2.6 presents a comparison between our proposed system and an existing underwater OCDMA system. Table 1 presents the evaluated values of the system parameters for the underwater wireless SAC-OCDMA system.

ISSN No:-2456-2165 https://doi.org/10.5281/zenodo.14637043

Table 1 Considered System Parameters of Underwater Wireless SAC-OCDMA System.

Electrical bandwidth (B_W)	**250 MHz [17]**
The spectral line width of the thermal source (Δw)	8 THz [17]
In response to the two APDs (r_e)	0.9
Both Si-APDs' gain (A)	120 [82]
The ionization factor (k_e)	0.02 [82]
The receiver's resistance to the load (rL)	100 □
The absolute temperature of the noise in the receiver (Tno)	298 K
The coupling efficiency of the receiver (ηrx)	0.9
Transmitter's coupling skills (ηtx)	0.9
Transmission wavelength of the optical source (λ)	532 nm
The electron's charge (q)	1.6×10^{-19} C
Major number of the MQC code (p)	7
The Boltzmann constant (k_C)	1.38×10^{-23} J/K
Electrical bandwidth (B_W)	250 MHz [17]

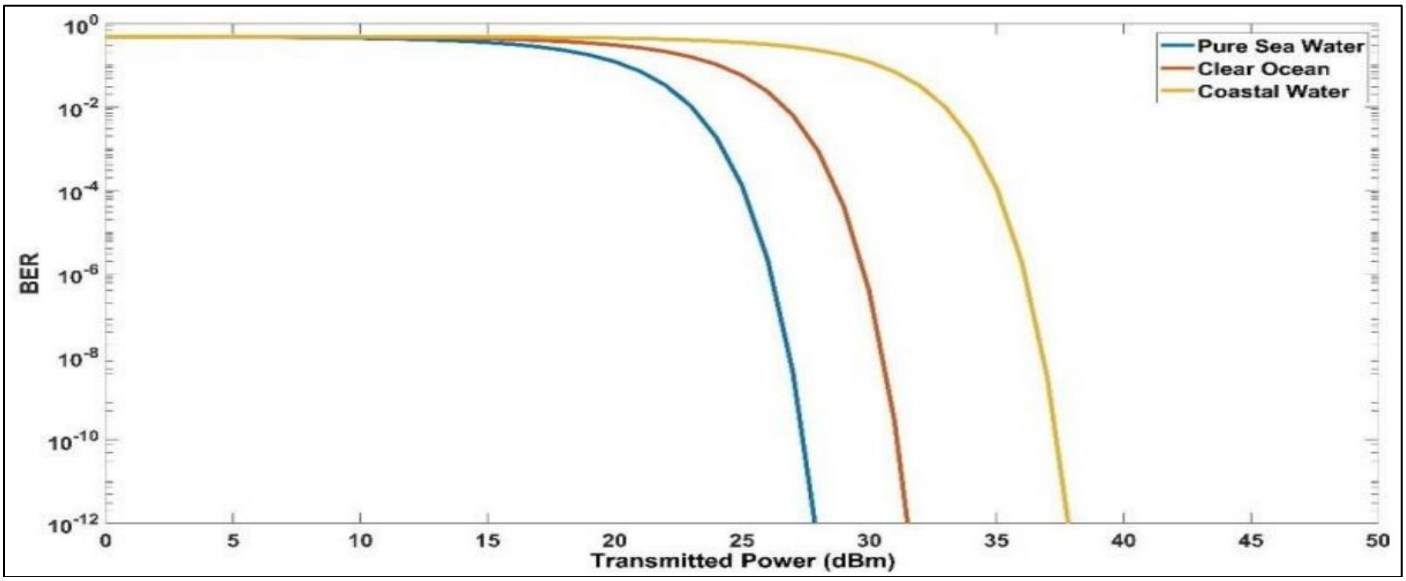

Fig 2 BER vs Photo Diode Transmitted Power There are twelve users concurrently when the link distance is 12 meters and the inclination angle is 10 degrees.

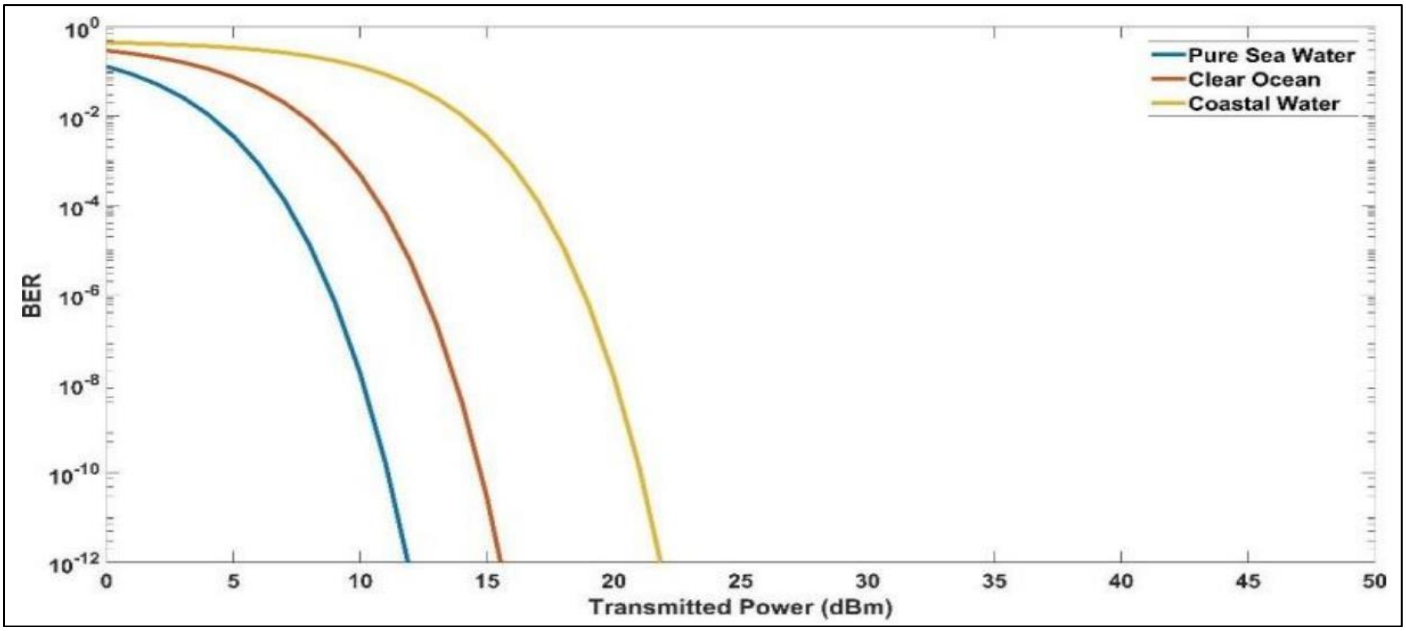

Fig 3 BER vs. Transmitted power (Avalanche Photo Diode) when the inclination angle is 10 degrees, the link distance is 12m, and number of simultaneous users is 12.

ISSN No:-2456-2165 https://doi.org/10.5281/zenodo.14637043

Bit Error Rate (BER) and transmitted power for photodiodes and avalanche photodiodes (APDs) under varied water conditions are shown in Figures 1 and 2. The study includes key factors including a 10^{-9}\ inclination angle, a 12-meter link distance, 12 simultaneous transmissions, and a prime number of 7. Both figures show BER decreasing with transmitted power. Photodiodes require transmission power of 27.08 dBm (pure seawater), 30.73 dBm (clear ocean water), and 37.05 dBm (coastal ocean water) to achieve a BER of \(10^{-9}\). However, APDs had far lower values at 10.46, 14.15, and 20.43 dBm. APDs appear to be more efficient, requiring less transmitted power to achieve the desired BER. They are advantageous in low-signal-strength conditions when traditional photodiodes fail to attain the required signal-to-noise ratio.

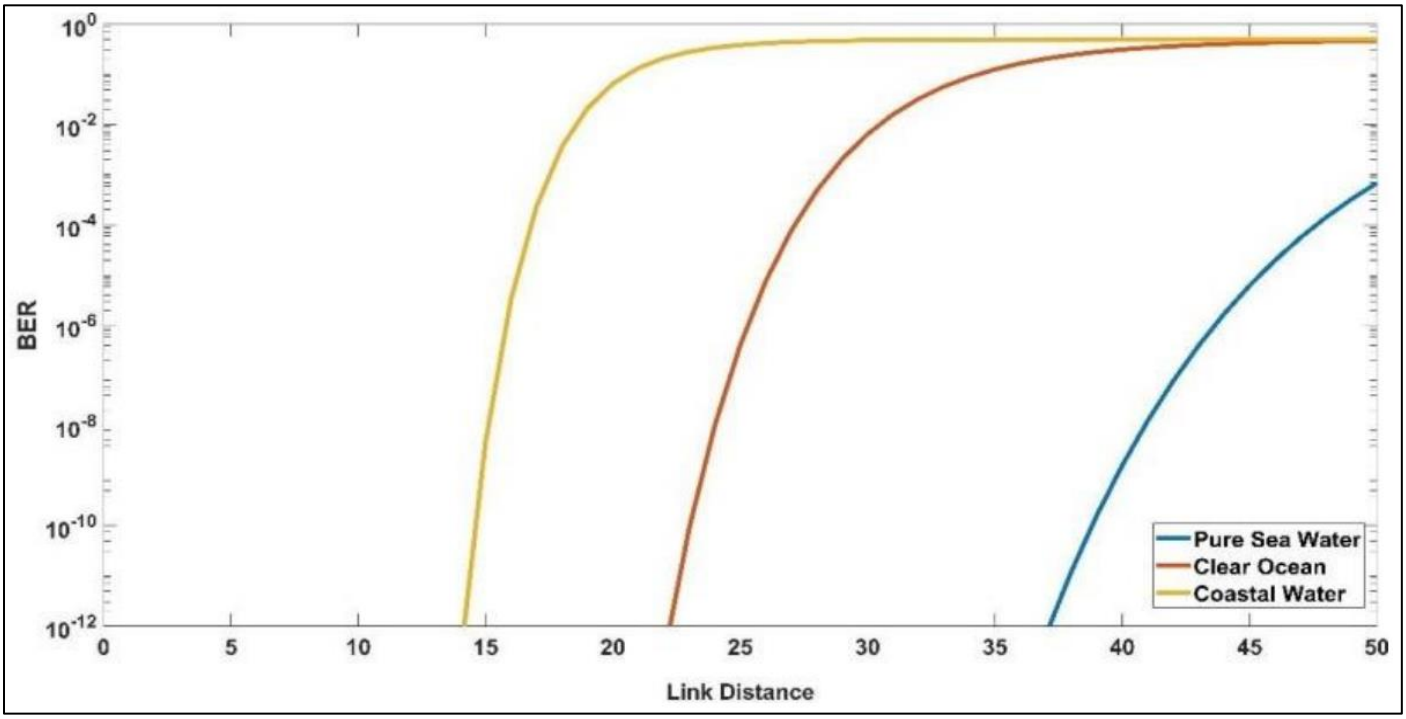

Fig 4 BER vs Link Distance (Photodiode) When the inclination angle is ten degrees and there are twelve simultaneous users, the transmitted power is 35 dBm.

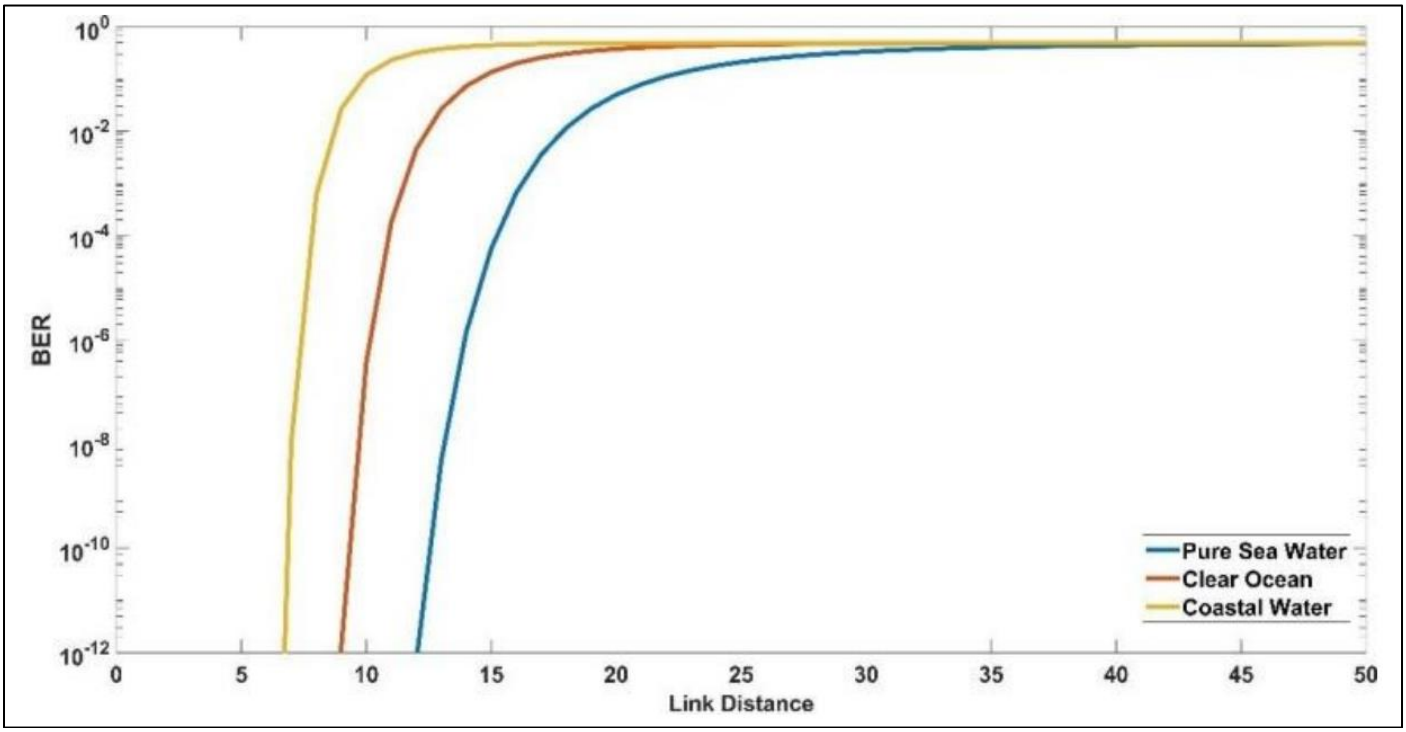

Fig 5 BER vs. Link distance (Avalanche Photo Diode) when inclination angle is 10-degree, number of simultaneous users are 12, transmitted power is 35 dBm.

ISSN No:-2456-2165 https://doi.org/10.5281/zenodo.14637043

Figure 3 illustrates the BER versus link distance for a photodiode, while Figure 4 presents the same for an avalanche photodiode (APD) under various water conditions, incorporating gain (A) and excess noise factor (fe) for the APD. Both figures are based on an inclination angle of 10 degrees, with 12 simultaneous users, a transmitted power of 35 dBm, and a prime number of 7. The photodiode demonstrates a bit error rate of \(10^{-9}\) at distances of 12.89 m in pure sea water, 9.582 m in clear ocean water, and 6.99 m in coastal ocean water. In comparison, the APD reaches the same BER at notably longer distances: 40.8 m, 23.65 m, and 14.91 m, respectively. The analysis reveals that APDs surpass photodiodes in deep water scenarios, attributed to their superior sensitivity and gain, which facilitate the identification of faint optical signals across long distances.

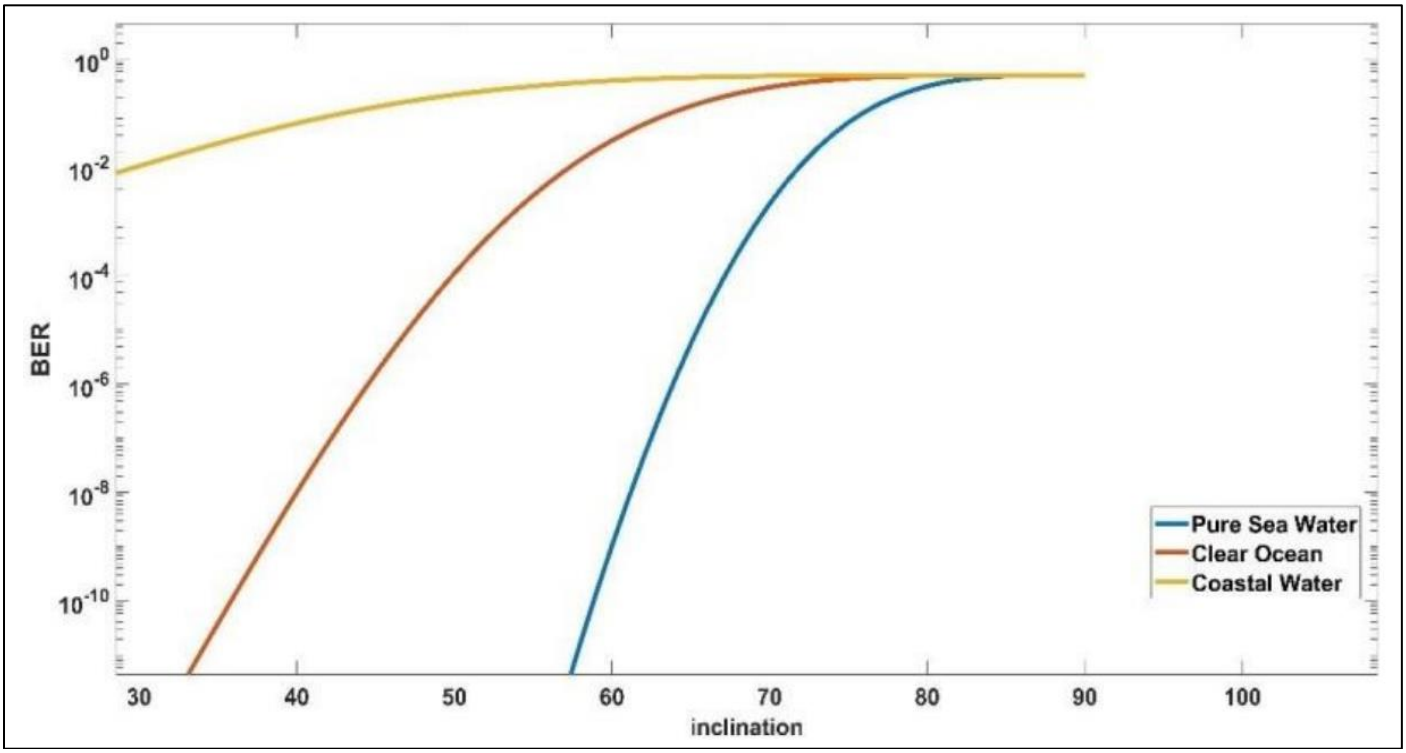

Fig 6 BER vs. Inclination angle (Photo Diode) when simultaneous users are 12, link distance is 12m, transmitted power is 35 dBm.

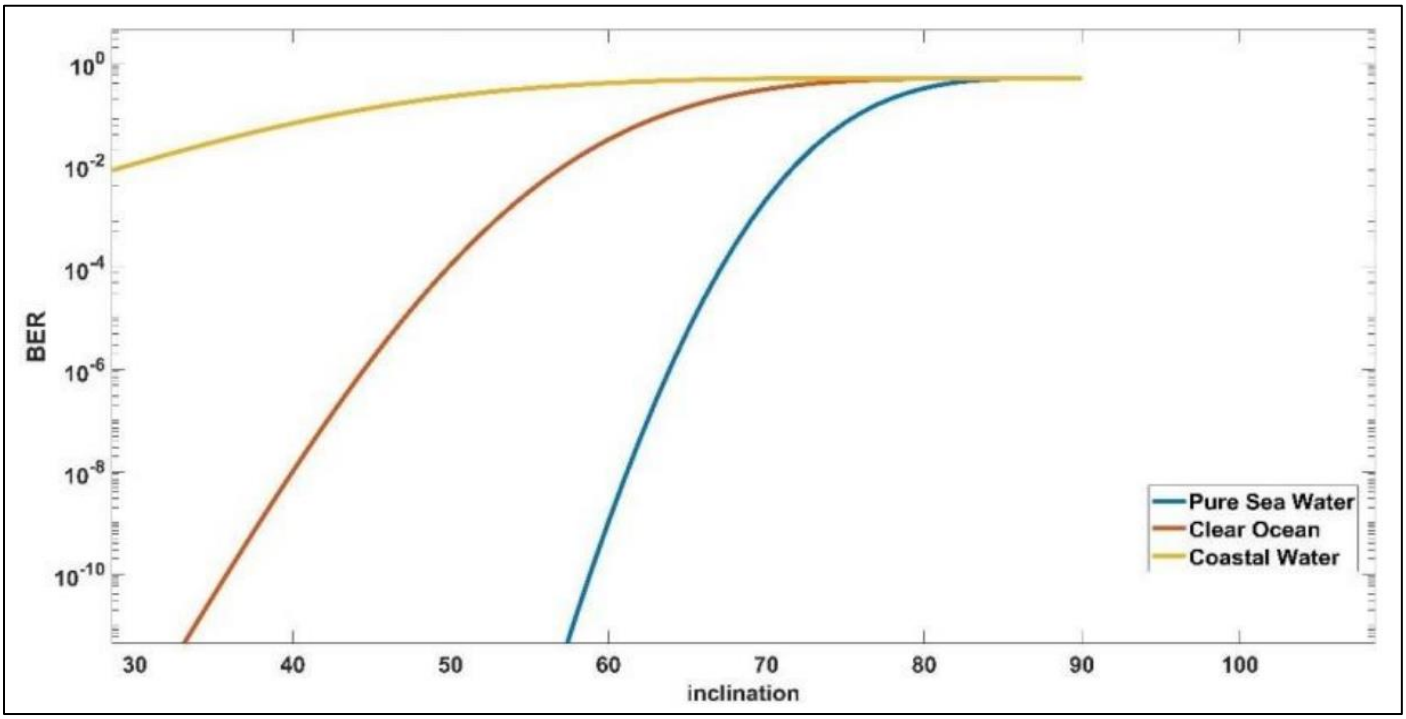

Fig 7 BER vs. Inclination angle (Avalanche Photo Diode) when simultaneous users are 12, link distance is 12m, transmitted power is 35 dBm.

ISSN No:-2456-2165 https://doi.org/10.5281/zenodo.14637043

Figure 5 and Figure 6 illustrate the comparison of Bit Error Rate (BER) against inclination angle for photodiodes as well as avalanche photodiodes (APDs) across different water conditions. The analysis is conducted with a transmitted power of 35 dBm, involving 12 simultaneous users, a length of 12 m, and utilizing a prime number of 7. The findings indicate that the bit error rate rises as the angle of inclination expands. In the case of photodiodes, bit error rate values of \(10^{-9}\) are achieved at inclination angles of 60.32°, 38.49°, and 20.62° when tested in pure seawater, clear ocean water, and coastal ocean water, respectively. For APDs, the identical BER is gained at 83.28°, 76.05°, and 64.66° under consistent conditions. The elevated inclination angles for APDs suggest their enhanced suitability for these applications, due to their superior gain, sensitivity, rapid response time, and reduced noise levels, which contribute to their effectiveness in high-speed communication within challenging underwater environments.

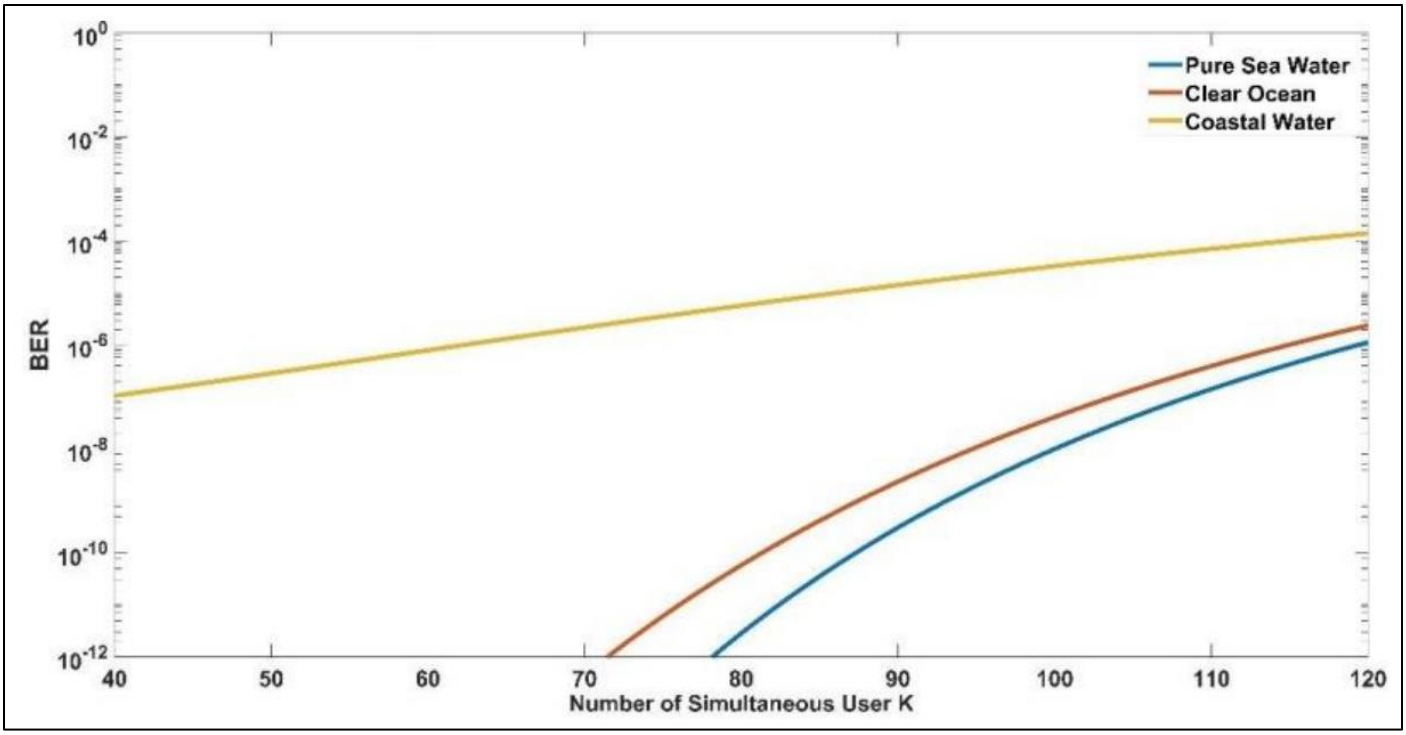

Fig 8 BER vs. Number of simultaneous users (Photo Diode) when inclination angle is 10-degree, link distance is 12m, transmitted power is 35 dBm.

Fig 7 and 8 present the BER with the number of simultaneous users for a photodiode and an avalanche photodiode (APD) across different water conditions, respectively. The analysis incorporates gain and excess noise factors for the APD, with specific parameters including a 10° inclination angle, a link distance of 12 m, and transmission strength of 35 dBm. The upper limit of users is defined by the prime number's squared value in the MQC code, permitting a maximum of 120 users when the bit error rate is 0.0001415. In pure sea water and clear ocean water, around 94 and 89 users can establish communication at a BER of \(10^{-9}\), whereas coastal ocean water accommodates 120 users at a BER of 0.0001415. Figure 2 shows similar trends, with APDs outperforming photodiodes by supporting more simultaneous users due to their higher sensitivity and capacity for handling high-speed underwater communications.

An analysis is conducted on the BER performance of an underwater OCDMA system that employs optical orthogonal codes as the signature code. This study emphasizes various factors, including channel length, the sum of simultaneous users, code weight, code length, and transmitted power, all while ensuring a BER of \(10^{-9}\). This study investigates a SAC-OCDMA system by analyzing various parameters such as transmission distance, turbulence, inclination angle, and beam divergence angle, employing the MQC code as the addressing sequence. The performance comparison of the two systems is thoroughly summarized in Table 2.

Table 2 Performance comparison between the current OCDMA system and the suggested SAC-OCDMA system via underwater link

Parameters	**Existing model [18]**	**Proposed model**
Coding technique	Optical orthogonal code	MQC code
Maximum No. of simultaneoususer in a single channel	42	Equal to p^2. If, p 11 then maximumno of users would be 121.
Inclination angle	10°	10°
Beam divergence angle	60°	35°

ISSN No:-2456-2165 https://doi.org/10.5281/zenodo.14637043

Coupling efficiency of the transmitter and receivers	0.8	0.9
Maximum Channel length for optimum performance	50 m in case of pure sea water	10-100 m
Load resistance	1000 Ω	100 Ω
Bandwidth	5 GHz	250 MHz
MUI	Moderate	Can be mitigated by deploying balanced detection technique
Security	High	Higher
Considered Constraints	Absorption and scattering	Absorption, scattering and turbulence

IV. CONCLUSION

This thesis introduces a wireless SAC-OCDMA system designed for underwater communication, utilizing MQC codes and examining its BER performance across different system parameters and environmental challenges. A system model utilizing a 532 nm LED optical source is presented, with its mathematical representation accounting for the influences of absorption, scattering, and turbulence. The evaluation of performance spans various types of seawater-showing the best results in pure seawater while indicating reduced performance in coastal waters. Significant observations indicate that BER rises alongside the number of users and the distance of the link, attributed to the absorption and scattered optical signals. For instance, in pure seawater, the BER is \(10^{-9}\) at a link distance of approximately 30.5 m but degrades to \(10^{-5}\) at 36.4 m. In a similar manner, the necessary optical power increases as the number of users, link distance, inclination angle, and beam divergence angle rise. The analysis incorporates oceanic turbulence effects through the Gamma-Gamma model, emphasizing the negative influence of RYTOV variance on BER. In clear ocean water, achieving a bit error rate of \(10^{-9}\) necessitates an increase in power from 23.11 dBm to 26.6 dBm as the intensity of turbulence rises. The investigation highlights approaches to enhance system efficiency in demanding underwater environments, stressing the importance of reducing beam divergence and controlling environmental influences.

FUTURE SCOPES

The present study is carried out on the execution of the SAC-OCDMA system for underwater wireless communication. Here, MQC codes are utilized as the order of addresses user . Also, the effect of photodiode and avalanche photodiode for different parameters. All analysis is done in three different types of water. Future analyses may consider the following subjects.

- OCDMA with asynchronous time can be used for more bandwidth utilization.
- Multi-dimensional coding schemes can be considered.
- Multi-wavelength optical CDMA (MW-OCDMA) system can be implemented for underwater wireless communication.
- FH-OCDMA system implementation and performance analysis

REFERENCES

[1]. Z. Zeng, S, Fu, H. Zhang,Y. Dong and J. Cheng, “A Survey of Underwater Wireless Optical Communication,” IEEE Communications Surveys & Tutorials, vol. 19, no.1, pp. 204 - 238, October 2016.

[2]. Y. Weng, Y. Guo, O. Alkhazragi, T. Khee Ng, J. Guo and B. S. Ooi, “Impact of Turbulent-Flow-Induced Scintillation on Deep-Ocean Wireless Optical Communication,” Journal of Lightwave Technology, vol. 37, no.19, pp. 5083 - 5090, July 2019.

[3]. M. Jouhari, K.Ibrahimi, H.Tembine and J. Ben-Othman, “Underwater Wireless Sensor Networks: A Survey on Enabling Technologies, Localization Protocols, and Internet of Underwater Things,” IEEE Access, vol. 7, pp. 96879 - 96899, July 2019.

[4]. R. Diamant, F. Campagnaro, M. D. F. D. Grazia, P. Casari, A. Testolin, V. S. Calzado and M.Zorzi, “On the Relationship Between the Underwater Acoustic and Optical Channels,” IEEE Transactions on Wireless Communications, vol. 16, no.12, pp. 8037 - 8051, December 2017.

[5]. G. N. Arvanitakis, R. Bian, J. J. D. McKendry, C. Cheng, E. Xie, X. He, G. Yang, M. S. Islim, Ardimas A. Purwita, E. Gu, H. Haas and M.D. Dawson, “Gb/s Underwater Wireless Optical Communications Using Series-Connected GaN Micro-LED Arrays,” IEEE Photonics Journal, vol. 12, no.2, 7901210, April 2020.

[6]. A. Al-Kinani, C. X. Wang, L. Zhou and W. Zhang, “Optical Wireless Communication Channel Measurements and Models,” IEEE Communications Surveys & Tutorials, vol. 20, no.3, pp. 1939 - 1962, 2018.

[7]. G. P. Agrawal, “FIBER-OPTIC COMMUNICATION SYSTEMS”, 4th Edition, pp. 135- 140.

[8]. H. Kaushal and G. Kaddoum, “Underwater optical wireless communication,” IEEE Access, vol. 4, pp. 1518-1547, 2016.

[9]. S. Gupta, A. Goel, “Advance Method for Security Enhancement in Optical Code Division Multiple Access System,’ IETE J. Research, vol. 64, pp. 17-26, 2017.

[10]. M. Najjar, N. Jellali, M. Ferchich, H. Rezig, “Spectral/Spatial optical CDMA code based on Diagonal Eigenvalue Unity,” J. Opt. Fiber Techn., vol. 38, pp. 61-69, 2017.